

Tetragonal and trigonal deformations in zinc-blende semiconductors : a tight-binding point of view

J.-M. Jancu¹ and P. Voisin¹

¹ *Laboratoire de Photonique et de Nanostructure,
CNRS, route de Nozay, F-91000 Marcoussis, France*

(Dated: July 22, 2021)

Abstract

The deformation potentials of cubic semiconductors are re-examined from the point of view of the extended-basis $sp^3d^5s^*$ tight-binding model. Previous parametrizations had failed to account properly for trigonal deformations, even leading to incorrect sign of the acoustic component of the shear deformation potential d . The strain-induced shifts and splittings of the on-site energies of the p- and d-orbitals are shown to play a prominent role in obtaining satisfactory values of deformation potentials both at the zone center and zone extrema. The present approach results in excellent agreement with available experimental data and ab-initio calculations.

PACS numbers: 71.15.Ap, 71.55.Eq, 73.21.La, 85.75.-d

The effect of uniaxial stress on the band structure of semiconductors has been a major theoretical and experimental topic for many years. With the development of strained-layer epitaxy, it has also become an important issue in modern material science and device physics. In their seminal approach, nearly half a century ago, Bir and Pikus established the strain Hamiltonian using the theory of invariants [1]. It depends on a number of deformation potentials describing the shifts and splittings of the various band extrema. For instance, for a given band near the Brillouin zone center, it reads as :

$$H_{\epsilon}^i = -a^i (\epsilon_{xx} + \epsilon_{yy} + \epsilon_{zz}) - 3b^i \left[\left(L_z^2 - \frac{1}{3}\mathbf{L}^2 \right) \epsilon_{zz} + c.p \right] - \frac{6}{\sqrt{3}}d^i [\{L_x L_y\} \epsilon_{xy} + c.p] \quad (1)$$

Where ϵ_{ij} are the components of the strain tensor, \mathbf{L} is the angular momentum operator, $\{L_x L_y\} = \frac{1}{2}(L_y L_x + L_x L_y)$, and c.p refers to circular permutations with respect to the axes x, y, z . The coefficient a^i is the hydrostatic deformation potential for the i th band, while b^i and d^i are respectively the tetragonal and rhombohedral (or trigonal) deformation potentials. We now explicit Eq. (1) for the Γ_6 and Γ_8 states of zinc-blende crystals : the Γ_6 conduction-band energy only depends on the hydrostatic term owing of the $L = 0$ matrix representation of the momentum operator. For the Γ_8 valence-band edge, the heavy- and light-hole degeneracy is lifted (as $L = 1$) and the splitting depends on the strain orientation. Under [001] uniaxial stress or for lattice mismatched epilayers grown along the [001] direction, strain components can be written as: $\epsilon_{xx} = \epsilon_{yy} \neq \epsilon_{zz}$ and $\epsilon_{xy} = \epsilon_{yz} = \epsilon_{zx} = 0$. Thus, the heavy- and light-hole bands split by an amount proportional to b . Under [111] stress or for mismatched epilayers grown along the [111] direction, we have $\epsilon_{xx} = \epsilon_{yy} = \epsilon_{zz} \neq 0$ and $\epsilon_{xy} = \epsilon_{yz} = \epsilon_{zx} \neq 0$, giving a valence-band splitting proportionnal to d . The two situations also differ by the presence or not of a static displacement of the anion and cation sublattices: in the former case all the atomic bonds in the strained crystal retain the same length and same angle with respect to the strain symmetry axis, giving no short range contribution to the strain hamiltonian. Conversely, for trigonal distortions, the equilibrium positions of atoms are no longer fully determined by stress invariants and a relative displacement of the sublattices is allowed. The resulting internal strain is represented by the Kleinmann parameter ζ which ranges between 0 and 1 [2]. The value $\zeta = 1$ corresponds a deformation with the same symmetry as the [111] strain but maintaining equal bond lengths of $a_0\sqrt{3}/4$, whereas $\zeta = 0$ is related to the macroscopic strain that does not account for sublattice

displacement. This gives simultaneously a long range or acoustic (d') and a short range or optical (d_0) contribution to the rhombohedral deformation potential d [3]:

$$d = d' - \frac{\zeta}{4}d_0 \quad (2)$$

The strain hamiltonian has been extensively used in connection with the $\mathbf{k}\cdot\mathbf{p}$ theory to interpret experimental data and measure parameters. On a more fundamental side, several *ab initio* calculations of the deformation potentials have been reported. More recently, atomistic approaches using empirical parameters have become a strong challenger to $\mathbf{k}\cdot\mathbf{p}$ theory for a precise modeling of semiconductor nanostructures where compositions and deformations can vary rapidly at the bond-length scale. A remarkable feature of atomistic theories (as opposed to the fundamentally perturbative character of the $\mathbf{k}\cdot\mathbf{p}$ theory) is their natural ability to treat the whole Brillouin zone. It follows that a "good" atomistic model must give a proper account of general distortions not only in the vicinity of the fundamental gap, but also at the edges of the Brillouin zone: the effects of strain actually is a very stringent test of atomistic models. Here we examine the effects of tetragonal and trigonal deformations from the point of view of the empirical tight binding (TB) theory.

Within the tight-binding formalism, strain effects are mainly determined by scaling the Slater-Koster two-center integrals [4] (or transfer integrals) with respect to bond-length alterations, while bond-angle distortions are automatically incorporated via the phase factors in the Slater-Koster matrix elements. This leaves a more than sufficient number of strain-dependent parameters to fit the deformation potentials at the Brillouin zone center. However, when trying to fit simultaneously the splitting of zone-edge conduction valleys, one encounters a difficulty. For the case of [001] uniaxial strain, it was shown in Ref. [6] that adding a term corresponding to a strain-induced splitting of the d -orbitals on-site energies (one-center integrals) leads to a much better overall fit of the deformation potentials at Γ and X . Indeed, since the Wannier functions of tight-binding models are Slater-type orbitals [5], the one-center integrals are expected to be sensitive to the environment of neighboring atoms. In principle, one should also introduce a [001] shear parameter of the on-site p energies, and this can be generalized to all diagonal matrix elements in proportion to cubic and uniaxial distortions. However, in the atomic limit, the on-site properties should depend neither on strain, nor on chemical environment. This is nearly the case for the s and p

valence states that display an excellent degree of transferability. Conversely, it is clear that the excited s and d -like orbitals have a strong free-electron character and corresponding energies must depend on strain-induced effects. Finally, one should remember that the "rule of the game" of atomistic models is to limit the number of empirical parameters to the minimum required to account for symmetries and reproduce experimental (or *ab initio*) band parameters within a given accuracy. For instance, the hydrostatic shift of on-site energies appeared to be useless parameters at the present level of model sophistication, as they are for a large part renormalized in the variation of transfer integrals with bond-length changes.

To the best of our knowledge, the case of trigonal deformations has never been discussed in the framework of an advanced tight binding model. A first difficulty is the choice of a value for the internal-strain parameter ζ : contrarily to *ab initio* calculations, the atomic positions are an input of the tight binding model, not a result of the calculation. ζ can be obtained theoretically either in *ab initio* calculations or from the fit of phonon dispersions, as first demonstrated by Nielsen and Martin [7]. ζ was precisely measured by X-ray diffraction for Si and Ge. The common value $\zeta = 0.54$ [8] is in agreement with first-principle calculations [7]. However, for GaAs, the most-cited experimental result $\zeta = 0.76$ [12] is still controversial [7, 9, 13, 14] and differs significantly from the theoretical value $\zeta = 0.48$ obtained by Nielsen and Martin [7]. Note that the latter value gives an excellent representation of elastic constants and phonon frequencies of GaAs and is corroborated by recent x-ray measurements which give $\zeta=0.55$ [9]. The second difficulty is methodological since a fit of d comes out of a calculation, while there are two quantities to determine, d' and d_0 . Here, d' is obtained by running the code using the fit parameters and setting $\zeta = 0$, whereas a relative displacement of the anion and cation sublattices in absence of macroscopic strain, is used to calculate d_0 .

The need for introducing a new shear parameter is evidenced by the failure of simpler tight-binding models : in the minimal sp^3 basis, the TB Hamiltonian cannot describe both b and d satisfactorily, as seen for the diamond structure where b , d' , and d_0 are linked by the analytical relations [3]:

$$d_0 = 16d' = -\frac{16}{\sqrt{3}}b \quad (3)$$

For Ge, fitting $b=-1.88$ eV ± 0.12 [10] and considering $\zeta = 0.54$, one obtain: $d=-1.26$ eV, in poor agreement with the experimental result: $d=-5.0 \pm 0.5$ eV [11]. The failure is mainly caused by an erroneous positive deformation potential d' (see Eq. 3) in sharp contrast with

the sign calculated by the self-consistent LMTO and *ab initio* pseudopotential approaches [13, 14] which show a strong redistribution of the valence-electron density induced by the acoustic deformation. Similar discrepancies are obtained numerically for the zinc-blende semiconductors and no significant changes appear within the $sp^3s^*d^5$ approach, until a splitting of on-site energies is introduced. The corresponding hamiltonian obviously depends on the strain direction. For a uniaxial stress along [001], the perturbation has the Γ_{12} symmetry, and the crystal field splits the fivefold degenerate d orbitals into two doublets and a singlet as :

$$\begin{aligned}
E_{d_{xz}} = E_{d_{yz}} &= E_d (1 - \delta_{001}(\epsilon_{zz} - \epsilon_{xx})) \\
E_{d_{x^2-y^2}} &= E_{d_{x^2-y^2}} = E_d \\
E_{d_{xy}} &= E_d (1 + 2\delta_{001}(\epsilon_{zz} - \epsilon_{xx}))
\end{aligned} \tag{4}$$

For a uniaxial strain along [111] the perturbation has the Γ_{15} symmetry and also splits the five equivalent d bands into two doublets and a singlet state. To handle this case, it is more convenient to rotate the coordinate system and choose the quantization axis \bar{z} along the [111] direction. To avoid confusions we name " (111) basis" the new ($\bar{x}, \bar{y}, \bar{z}$) basis.

The on-site d energies now corresponds to the representations A_1 with $E_{d_{3\bar{z}^2-r^2}}$, E_1 with $E_{d_{\bar{x}\bar{z}}}$ and $E_{d_{\bar{y}\bar{z}}}$, and E_2 with $E_{d_{\bar{x}^2-\bar{y}^2}}$ and $E_{d_{\bar{x}\bar{y}}}$:

$$\begin{aligned}
E_{d_{3\bar{z}^2-r^2}} &= E_d (1 + 2\delta_{111}(\epsilon_{\bar{z}} - \epsilon_{\bar{x}})) \\
E_{d_{\bar{x}\bar{z}}} = E_{d_{\bar{y}\bar{z}}} &= E_d (1 - \delta_{111}(\epsilon_{\bar{z}} - \epsilon_{\bar{x}})) \\
E_{d_{\bar{x}^2-\bar{y}^2}} &= E_{d_{\bar{x}\bar{y}}} = E_d \\
\epsilon_{\bar{z}} - \epsilon_{\bar{x}} &= \frac{8}{3}(1 - \zeta)\epsilon_{xy}
\end{aligned} \tag{5}$$

Negative ϵ_{xy} corresponds to conventional compressive stress. δ_{001} and δ_{111} are shear parameters fitted to reproduce the tetragonal and trigonal deformation of the valence-band edge, respectively. Note that, since perturbations result from different modifications of the nearest neighbors positions, there is no reason for an exact geometrical relation linking δ_{001} and δ_{111} . The scheme of level splittings for uniaxial compressions along [001] and [111] is shown in figure 1. Following this procedure, we demonstrate excellent agreement with

experiment for b and d . In addition, the figures coming out for the acoustic deformation potential d' are consistent with self-consistent LMTO results [13]. For instance, for Ge, using the parametrization of Ref. [6], with $\delta_{001}=0.54$ and $\delta_{111}=-1.5$, we get: $b=-1.9$ eV, $d=-4.6$ eV, and $d'=-1.37$ eV, in agreement with experiment: $b=-1.88 \pm 0.12$ eV [10], $d=-5.0$ eV ± 0.5 [11], and the LMTO calculation: $d'=-1.3$ eV [13].

Furthermore, as discussed in Ref. [6], introduction of δ_{001} allows to obtain simultaneously a fit of b and of the conduction-band splitting of X valleys under [001] stress. However, for [111] stress, when examining the shear deformation potential of the L_1 conduction extrema, using our fit value of δ_{111} , we find a very large and disappointing discrepancy: $D_1^{5c}=12.5$ eV, to be compared to the experimental value of 18.3 eV [11]. This witnesses that there is still a missing parameter to describe properly the effects of trigonal deformations. From a quantum chemistry point of view, this discrepancy can be understood from the fact that the L -conduction band minimum is dominated by s and p states, in contrast with wavefunctions at X that have a strong d character [6]. Therefore, the splitting of on-site d energies cannot help much to fit the strain deformation potential at L . Instead, the splitting of on-site p energies, which was up to now a non-necessary parameter, becomes important to model strain field anisotropies. At this point, the internal logic of the model implies that if the strain induced splittings of the one-center integrals play such an important role, their shift under hydrostatic strain should also be taken explicitly into account instead of being renormalized in a strain dependency of two-center integrals. Using again the "(111) basis", the corresponding contributions to (111)-strain hamiltonian are written as:

$$\begin{aligned} E_{p_{\bar{x}}} &= E_{p_{\bar{y}}} = E_p (1 - \pi_{111}(\epsilon_{\bar{z}} - \epsilon_{\bar{x}})) \\ E_{p_{\bar{z}}} &= E_p (1 + 2\pi_{111}(\epsilon_{\bar{z}} - \epsilon_{\bar{x}})) \end{aligned} \quad (6)$$

The values of d , d' , d_0 , and D_1^{5c} , for Ge and GaAs semiconductors are compared in table 1 with available experimental data and LMTO [13] evaluations. We use values of ζ issued from experiments and fit π_{111} and δ_{111} to reproduce the trigonal deformation of the valence-band edge and L -conduction band valleys. To achieve a complete description of strain effects in the $spds^*$ model, on-site Hamiltonian matrix elements were also scaled with respect to bond-length changes resulting. Although the number of tight-binding parameters is increased with respect of Ref [6] their numerical determination through

a multi-parameter fitting procedure still converges very well and resulting values gain a more intuitive view of chemical dependences. A detailed description of the complete parametrization is beyond the scope of the present work and will be the subject of a forthcoming paper. The data presented in Table 1 demonstrate that our results are in good agreement with experimental and theoretical values for d and D_1^{5c} . The magnitude and sign of d' and d_0 are well reproduced compared to the LMTO calculations. Our values for d_0 differ from the experimental results whose values are actually controversial, a discrepancy observed already earlier; (compare Table 1).

In conclusion, we have demonstrated that the $sp^3d^5s^*$ model requires diagonal matrix element shifts to correctly reproduce uniaxial [klm] strain for cubic semiconductors. In order to test our model we have calculated the acoustic and optical contributions to the trigonal deformation potentials and found a good agreement with experiment and LMTO results. A major improvement compared to smaller TB models was the correct sign and magnitude of the acoustic deformation potential d' directly related to the shear parameter of d -states. This TB model provides a valid framework for the calculation of strain effects in self-assembled quantum dots.

Acknowledgments

The authors thank F. Glas for clarifying discussions.

-
- [1] G. L. Bir and G. E. Pikus, *Symmetry and Strain-Induced Effects in Semiconductors* (Wiley, New York, 1974).
 - [2] L. Kleinmann Phys. Rev. **128**, 2614 (1962)
 - [3] A. Blacha, H. Presting, and M. Cardona, Phys. Status Solidi B, **126**, 11 (1984).
 - [4] J. C. Slater and G. F. Koster, Phys. Rev. **94**, 1498 (1954).
 - [5] W. Kohn, Phys. Rev. B **10**, 4388 (1973).
 - [6] J.-M. Jancu, R. Scholz, F. Beltram, and F. Bassani, Phys. Rev. B **57**, 6493 (1998).
 - [7] O. H. Nielsen and R. M. Martin Phys. Rev Lett. **50**, 697 (1983), O. H. Nielsen and R. M. Martin, Phys. Rev B **32**, 3792 (1985); O. H. Nielsen, *ibid*, **34**, 5808 (1986).

- [8] C. S. G. Cousins, L. Gerward, J. Staun Olsen, B Selsmarck, and B. J. Sheldon, *J. Phys. C* **20**, 29 (1987).
- [9] C. S. G. Cousins, L. Gerward, J. Staun Olsen, B. Selsmark, B. J. Shedlon and G. E. Webster, *J. Semicond. Sci. Technol.* **4**, 333 (1989).
- [10] J. Liu, D. D. Cannon, K. Wada, Y. Ishikawa, D. T. Danielson, S. Jongthammanurak, J. Michel, and L. C. Kimerling, *Phys. Rev. B* **70**, 155309 (2004)
- [11] *Semiconductors: Group IV Elements and III-V Compounds*, edited by O. Madelung, Landolt-Brnstein, New Series, Group III, Vol. 17, Pt. a (Springer, Berlin, 1982); *Semiconductors: Intrinsic Properties of Group IV Elements and III-V, II-VI and I-VII Compounds*, edited by O. Madelung, Landolt-Brnstein, New Series, Group III, Vol. 22, Pt. a (Springer, Berlin, 1987).
- [12] C. N. Koumelis, G. E. Zardas, C. A. Londos, and D. K. Leventuri, *Acta Crystallogr. Sec. A* **32**, 84 (1975).
- [13] L. Brey, N. E. Christensen and M. Cardona, *Phys. Rev B* **36**, 2638 (1987).
- [14] Z.-Q. Gu, M.-F. Li, J.-Q. Wang and B.-S. Wang, *Phys. Rev B* **41**, 8333 (1990).

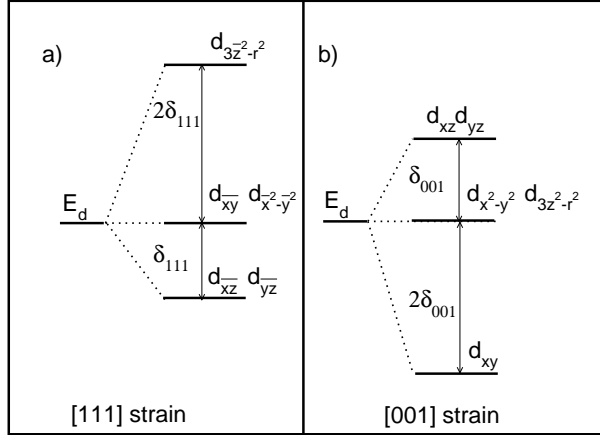


FIG. 1: Schematic plot of energy-level splitting of d states induced by an uniaxial strain along the [111] (left panel) and [001] directions (right panel). For [111] strain, the quantization axis \bar{z} is chosen along the [111] direction.

TABLE I: Comparison of trigonal deformation potentials obtained in present work with LMTO and experimental results. We use $\zeta = 0.54$ for Ge and $\zeta = 0.55$ for GaAs.

	Ge				GaAs			
	d_0	d'	d	D_1^{5c}	d_0	d'	d	D_1^{5c}
this work	30	-0.9	-5.0	17.1	27	-0.8	-4.5	18.0
LMTO ^a	22.4	-1.3	-5.0		25	-0.99		
Expt. ^b	33		-5.0	18.4	44		-4.5	20.8

^a Ref. [13], ^b Landolt-Börnstein Ref. [11].